Probing Bardeen-Cooper-Schrieffer Pairing and Quasiparticle Formation in Ultracold Gases by Rydberg Atom Spectroscopy

Emilio Ramos Rodríguez,[1,2] Marcel Gievers,[3] and Richard Schmidt[1]
[1]Institut für Theoretische Physik, Universität Heidelberg, 69120 Heidelberg, Germany
[2]Université Paris Cité, Laboratoire Matériaux et Phénomènes Quantiques (MPQ), CNRS, F-75013, Paris, France
[3]Institute of Solid State Physics, TU Wien, 1040 Vienna, Austria

(Received 24 November 2025; revised 1 April 2026; accepted 28 April 2026; published 16 June 2026)

Locally probing pairing in fermionic superfluids, ranging from micro- to macroscopic scales, has been a long-standing challenge. Here, we investigate a new approach that uses Rydberg impurities as a spectroscopic sensor of the surrounding strongly correlated state of ultracold paired fermions. The extended wave function of the Rydberg electron induces a finite-range potential that can bind atoms from the BCS medium, forming molecular states. As a consequence, the optical absorption spectrum of the impurity encodes key many-body properties. Using the functional determinant approach, we provide a direct measure of the superfluid gap through frequency shifts of dimer and trimer peaks. The spectra also reveal whether the Cooper pairs are broken or trapped intact. For static Rydberg atoms, we relate this signature of pairing to the suppression of the orthogonality catastrophe due to the superconducting gap resulting in the formation of well-defined polaron quasiparticles. Our Letter establishes Rydberg atom spectroscopy as a powerful local probe of strongly correlated matter.

DOI: 10.1103/3js1-2zc1

Recent advances in ultracold atom experiments have opened new pathways for exploring quantum many-body phenomena with unprecedented precision and in a controlled setting [1]. Among these, paired two-component fermionic systems, such as described by Bardeen-Cooper-Schrieffer (BCS) theory [2], remain a cornerstone of condensed matter physics. The central mechanism of the BCS theory, namely, the formation of Cooper pairs, underpins the emergence of superconductivity, where fermions undergo pairing to form a collective quantum state. However, despite the theoretical simplicity of BCS theory, existing experimental probes are limited to global, spatially averaged measurements [3–5], so directly probing the internal structure and dynamics of Cooper pairs remains an experimental challenge.

In solid-state systems, advances in local sensing, such as nitrogen-vacancy centers in diamonds [6,7], have enabled access to the properties of material samples from the macroscopic down to the nanometer scale [8]. These methods provide insight into correlated phases by converting many-body effects into measurable quantities of a controlled quantum sensor.

Published by the American Physical Society under the terms of the Creative Commons Attribution 4.0 International license. Further distribution of this work must maintain attribution to the author(s) and the published article's title, journal citation, and DOI.

In ultracold atomic systems, the search continues for local probes that can combine microscopic spatial resolution with the ability to measure spectral features of their quantum environment [9–11]. Among these, Rydberg atoms have emerged as promising candidates for such local spectroscopic probes. Rydberg atoms, which are characterized by highly excited electronic states and a spatial extent of hundreds of nanometers [12], induce a finite-range potential in their environment (cf. Fig. 1). Through a tunable scattering process, particles from the environment can bind to the Rydberg atom at the Rydberg radius r_{Ryd}, forming ultralong-range Rydberg molecules [13–16]. These exotic bound states have been proposed as microscopic probes for the spectral properties of a Bose-Einstein condensate [17], Fermi gases [18], and polaron formation [19]. In addition, for a one-dimensional system in equilibrium, the effect of a Rydberg impurity on the spatial dependence of the BCS gap parameter has been studied [20,21].

In this Letter, we describe how a heavy Rydberg impurity can be introduced to examine the local properties of paired superfluids (cf. Fig. 1). For this, we extend the application of the functional determinant approach [22,23] to anomalous fermion operators to obtain the absorption spectrum of the impurity. We show how each molecular absorption peak is generated by the breaking [cf. Figs. 1(a) and 1(c)] or trapping [cf. Fig. 1(b)] of a Cooper pair. The energy cost of breaking a Cooper pair allows for the measurement of the superconducting gap through shifts in the spectral peaks.

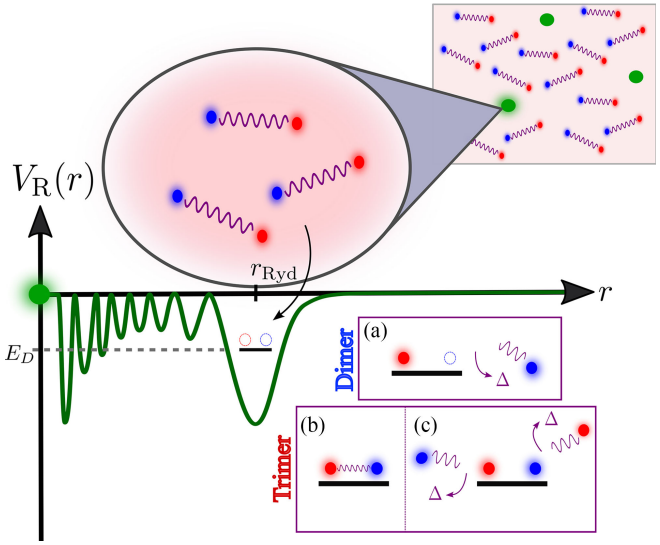


FIG. 1. Illustration of a Rydberg atom immersed in a BCS superfluid. The Rydberg potential $V_R(\boldsymbol{r})$ [Eq. (2)] is depicted by the green curve and Cooper pairs by red and blue circles connected by a wiggly purple line. A dimer (a) is formed after breaking a Cooper pair with the energy cost of the gap Δ. A trimer is formed by either (b) binding a whole Cooper pair or (c) breaking two Cooper pairs with an energy cost of 2Δ.

Because of the large scale separation, Rydberg sensing allows one to probe superfluid dynamics locally resolved and on ultrafast timescales. Strikingly, we find that Rydberg impurities can be used to study the orthogonality catastrophe (OC) and quasiparticle formation in the long-time domain. The OC typically presents itself in heavy-impurity systems, where multiple particle-hole excitations lead to a Fermi edge and power-law decay of the spectrum [24–26]. However, a gapped dispersion at the Fermi energy suppresses these excitations, essentially inducing an IR cutoff and enhancing quasiparticle formation [27]. Here, we show how the suppression of the OC allows us to verify intact trapping in the trimer state and quantify the dynamical transition into the quasiparticle regime from short- to long-time scales. With this method, one can combine the long-time dynamics of an impurity in a BCS state [28,29] with the microscopic probing of individual Cooper pairs in a single experiment.

Model—We consider a three-dimensional Fermi gas with two spin components denoted by $\sigma = \{\uparrow, \downarrow\}$. The pairing between the components is modeled within the mean-field BCS approximation [2]. The BCS Hamiltonian $\hat{H}_0$, without an impurity, takes the form ($\hbar = 1$)

$$\hat{H}_0 = \int_{\boldsymbol{r}} \hat{c}_{\boldsymbol{r}}^\dagger \begin{pmatrix} \hat{h}_\uparrow & \Delta \\ \Delta & -\hat{h}_\downarrow \end{pmatrix} \hat{c}_{\boldsymbol{r}} + E_g, \tag{1}$$

where $\hat{h}_\sigma = -\boldsymbol{\nabla}^2/(2m_\sigma) - \mu_\sigma$, μ_σ is the chemical potential, and m_σ is the mass of the σ component. Furthermore, we employ the Nambu spinor representation $\hat{c}_{\boldsymbol{r}}^\dagger = (\hat{c}_{\uparrow\boldsymbol{r}}^\dagger, \hat{c}_{\downarrow\boldsymbol{r}})$, where $\hat{c}_{\uparrow\boldsymbol{r}}^\dagger$ ($\hat{c}_{\downarrow\boldsymbol{r}}$) is the creation (annihilation) operator for a $\uparrow$ ($\downarrow$) fermion at position $\boldsymbol{r}$. The gap $\Delta \in \mathbb{R}^+$ represents the s-wave BCS order parameter. Note that Δ is a single-particle gap parameter in the weak-coupling regime. For strong coupling, however, it refers to the binding energy of tightly bound fermion pairs. The constant E_g arises from the Nambu representation and the mean-field ground state energy (see Supplemental Material [30]).

To introduce the impurity, we consider the following scheme. Initially, the impurity resides in a noninteracting electronic ground state $|0\rangle$, leaving the BCS host system in equilibrium. The impurity is then optically excited to a Rydberg state $|\mathrm{R}\rangle$. Here, the excited electron generates a static potential [13,35]:

$$V_\mathrm{R}(\boldsymbol{r}) = \frac{2\pi a_e}{m_e} |\psi_{n_\mathrm{Ryd}}(\boldsymbol{r})|^2, \tag{2}$$

with a_e the electron-neutral atom scattering length, m_e the electron mass, and $\psi_{n_\mathrm{Ryd}}(\boldsymbol{r})$ the wave function of the electron in a Rydberg state in an s-wave shell with principal quantum number n_Ryd.

The Hamiltonian for the impurity-BCS system is given by

$$\hat{H} = |0\rangle\langle 0| \otimes \hat{H}_0 + |\mathrm{R}\rangle\langle \mathrm{R}| \otimes \hat{H}_\mathrm{R}, \tag{3}$$

where

$$\hat{H}_\mathrm{R} = \int_{\boldsymbol{r}} \hat{c}_{\boldsymbol{r}}^\dagger \begin{pmatrix} \hat{h}_{\uparrow,\mathrm{R}} & \Delta \\ \Delta & -\hat{h}_{\downarrow,\mathrm{R}} \end{pmatrix} \hat{c}_{\boldsymbol{r}} + \tilde{E}_g, \tag{4}$$

with $\hat{h}_{\sigma,\mathrm{R}} = \hat{h}_\sigma + V_\mathrm{R}(\boldsymbol{r})$. Here, $\hat{H}_\mathrm{R}$ describes the BCS state in the presence of the Rydberg potential $V_\mathrm{R}(\boldsymbol{r})$; $\hat{h}_{\sigma,\mathrm{R}}$ is the corresponding single-particle operator, and $\tilde{E}_g$ accounts for the introduction of Eq. (2).

Following the excitation, the absorption spectrum $A(\omega)$ is measured. Because of its optical nature, the timescale of the excitation can be assumed to be much shorter than the equilibration time between the superfluid and the impurity [18,36,37], ensuring that the order parameter Δ remains homogeneous in the vicinity of the impurity during the procedure. The contribution of inhomogeneities in the BCS superfluid to the sudden absorption signals can, thus, be neglected. We note that recently, in a BCS medium, the backreaction of a Rydberg atom on the spatial dependence of the gap parameter and density has been analyzed for a one-dimensional system [20,21] whose size scarcely exceeds the Rydberg atom. Here, we focus on the experimentally relevant case where the dynamics follows a sudden excitation [18,19,38], i.e., where the BCS state does not equilibrate with the Rydberg atom. To this end,

we consider the out-of-equilibrium dynamics of a three-dimensional configuration with a large system size and compute the actual optical absorption spectra.

To obtain the absorption spectrum, we start by calculating the Ramsey signal [22]

$$S(t) = \mathrm{Tr}\{\hat{\rho}\, e^{i\hat{H}_0 t} e^{-i\hat{H}_R t}\}, \tag{5}$$

which quantifies the time-resolved overlap between many-body states with and without the Rydberg potential whose direct measurement has been demonstrated in both neutral [38] and Rydberg atoms [37,39]. In Eq. (5), $\hat{\rho} = e^{-\beta\hat{H}_0}/\mathrm{Tr}\{e^{-\beta\hat{H}_0}\}$ is the thermal density matrix and $\beta = 1/T$ the inverse temperature.

From here, the absorption spectrum follows as [22]

$$A(\omega) = 2\,\mathrm{Re}\left\{\int_0^\infty \mathrm{d}t\, S(t) e^{i\omega t}\right\}. \tag{6}$$

To compute $S(t)$, we employ the functional determinant approach (FDA) [22,31,40], reducing the problem to a single-particle description. We adapt the FDA to the BCS state and numerically solve the Schrödinger equation with and without the Rydberg potential by applying the Bogoliubov transformation [30]. While FDA can be directly used for finite temperature, the following results are all given for $T = 0$.

Rydberg atom spectroscopy—Motivated by experimental setups [41–44], we examine a Rydberg atom of ^{87}Rb that interacts with a two-component ^{40}K gas (BCS medium). This setting is experimentally realizable due to the separation of the Feshbach resonances of ^{40}K-^{40}K and ^{40}K-^{87}Rb scattering [45,46]. For numerical results, the electron of the ^{87}Rb atom is excited to the $n_{\mathrm{Ryd}} = 60$ level and characterized by a scattering length $a_e = -15a_0$ [47], with a_0 the Bohr radius. Although our model also generalizes to imbalanced configurations, we consider here the density balanced scenario where $\mu = \mu_\uparrow = \mu_\downarrow$ and $m = m_\uparrow = m_\downarrow$ at a background density of $\rho_0 = 5 \times 10^{11}$ cm^{-3} with $\epsilon_F \sim 1.2$ kHz.

For precision sensing of the BCS state, first a reference spectrum has to be established. This is shown in Fig. 2(a), where we consider the absorption spectrum in the absence of interactions, $\Delta = 0$, which is in agreement with data from previous research [18,19]. The general structure is characterized by several absorption peaks at negative frequencies. Each peak corresponds to the occupation of a bound state given by the potential $V_R(\boldsymbol{r})$. In our numerical

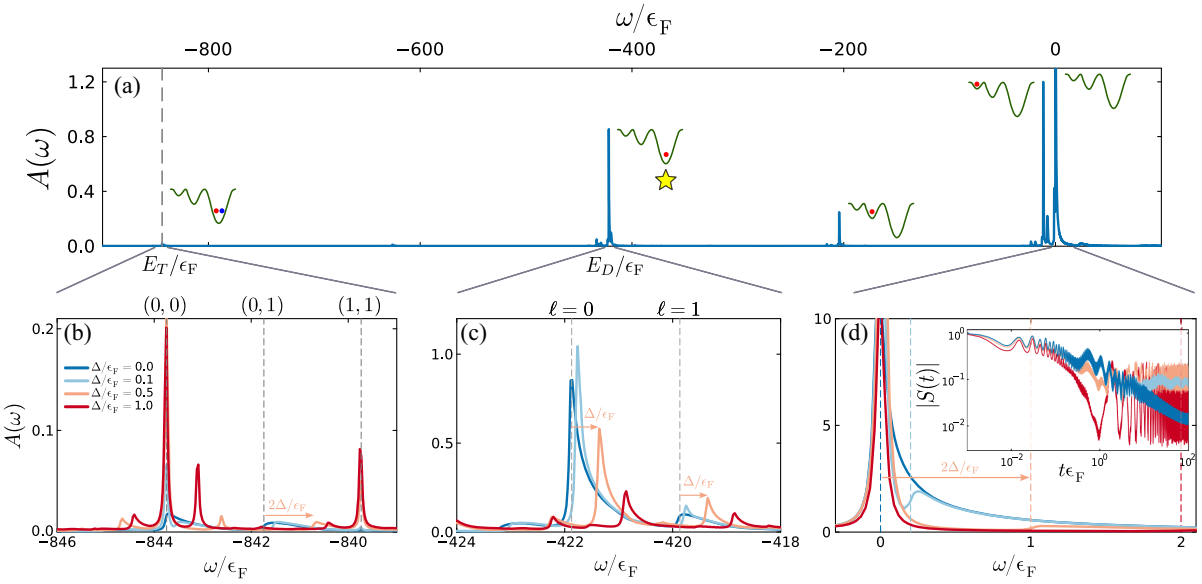


FIG. 2. Rydberg atom spectroscopy. (a) Absorption spectrum for $\Delta = 0$, where each peak corresponds to the occupation of a bound state in the Rydberg potential. The energy scale is shifted such that the bare atomic Rydberg peak is at the origin. (b)–(d) study the dependence of the spectrum on the gap parameter Δ (light blue to red curves). (b) Magnification of the trimer state, i.e., the double occupation of the bound state. Dashed lines mark the energies of different angular-momentum states of the bound state, denoted by $\ell = (\ell_1, \ell_2)$. Peaks with mixed angular momentum feature a shift of 2Δ, indicating the rupture of two Cooper pairs. Peaks with the same angular momentum do not show such a shift indicating intact trapping of the Cooper pair. (c) Dimer state: single occupation of the bound state for different angular momenta (dashed lines). All peaks shift proportional to the gap strength Δ, resulting in a direct measure of the superfluid gap, $\Delta = |E_D^{(\Delta)} - E_D|$. (d) Atomic Rydberg peak (repulsive branch): for $\Delta = 0$, the orthogonality catastrophe is present as seen from the power-law decay of the spectrum. This feature deforms into a δ-like peak structure for increasing gap strength accompanied by the appearance of a secondary branch corresponding to a Bogoliubov excitation. Inset: Ramsey signal for each gap strength showing the emergence of quasiparticle behavior.

calculations [30], each scattering channel hosts up to three two-body bound states. The finite-range nature of the potential sets an upper bound for the angular momentum that must be considered; here, $\ell \leq \ell_{\max} = 5$.

Our discussion of the local and time-resolved probing of the BCS state focuses on the outermost bound state, corresponding to the deepest well located at r_{Ryd} as depicted in Fig. 1 and marked by a yellow star in Fig. 2(a). We refer to the single occupation of this bound state as the *dimer* state. For $n = 60$, in the s-wave channel, it has a binding energy of $E_D \approx -421.9\epsilon_{\mathrm{F}}$; see Fig. 2(a). The double occupation of the bound state, the *trimer* state, then has an energy of $E_T = 2E_D$; peak at the dashed line in Fig. 2(a). For a complete analysis of each peak in the spectrum, including, in particular, those not discussed below, we refer to Supplemental Material [30].

Let us analyze how the spectrum is modified in the presence of the BCS state, i.e., $\Delta > 0$. The dimer peak for different values of the gap Δ is shown in Fig. 2(c). The vertical dashed lines, from left to right, correspond to the angular momentum states of the particle occupying the bound state, $\ell = 0$ and $\ell = 1$, respectively. As the superconducting gap increases, the $\ell = 0$ peak shifts from its value E_D in the absence of Δ to higher frequencies, denoted as $E_D^{(\Delta)}$. This represents a general feature of the dimer peak, also observed for the $\ell = 1$ state. The single occupation originates from the rupture of a Cooper pair to form the bound state. As the gap increases, so does the binding energy of the Cooper pair. Thus, the impurity requires more energy to trap a single particle of the medium. Indeed, the shift we find is precisely the gap Δ, such that

$$\Delta \approx \left| E_D^{(\Delta)} - E_D \right|. \tag{7}$$

This spectral feature, thus, allows one to measure the gap locally using focused laser light. Note that, because the Rydberg atom remains out of equilibrium with the BCS medium, through spatially distributed measurements, it is possible to reconstruct the spatial dependence of the gap parameter $\Delta(x)$.

The trimer state [cf. Fig. 2(b)] offers richer physics. The figure displays three dashed lines, representing the angular momenta of the two particles occupying the bound state, denoted by (ℓ_1, ℓ_2). Similarly to the dimer state, peaks corresponding to states with mixed angular momenta, e.g., (0,1), exhibit a shift of 2Δ. Strikingly, peaks associated with states where both particles share the same angular momentum, e.g., (0,0) and (1,1), do not shift as the superfluid gap Δ increases.

In the first case, the bounded particles with different angular momenta originate from the rupture of two Cooper pairs, as reflected by the 2Δ shift. However, an intact Cooper pair can also bind to the impurity as a whole. In this case, the trapping of the Cooper pair does not require an energy cost beyond the Rydberg molecular energy. As a result, this process is independent of the binding energy of the Cooper pair and will not lead to a shift in the spectrum, as seen in Fig. 2(b). Remarkably, we find that Cooper-pair trapping occurs even when its coherence length, $\xi(\Delta/\epsilon_{\mathrm{F}}) \approx \hbar v_{\mathrm{F}}/\Delta$, is greater than the diameter of the Rydberg potential, e.g., $\xi(\Delta/\epsilon_{\mathrm{F}} = 0.1) \sim 2.06\,\mu\mathrm{m} > 2r_{\mathrm{Ryd}} \sim 0.711\,\mu\mathrm{m}$. Here, ξ represents only the scale for the spatial decay of the Cooper-pair wave function. We attribute this observation to the three-dimensional geometry. In contrast to the one-dimensional analysis in Refs. [20,21], Cooper pairs can be aligned in multiple ways around the spherical surface defined by the Rydberg radius r_{Ryd}. Our results, thus, demonstrate that Cooper pairs can be trapped without disrupting its coherence. Moreover, Figs. 2(b) and 2(c) suggest that the spectral weight of the trimer peak increases with the gap strength, while the spectral weight of the dimer peak decreases. Accordingly, it is more probable that Cooper-pair trapping occurs when ξ is smaller, whereas for larger ξ, Cooper-pair breaking is preferred. In order to further investigate this mechanism, one could study how the wave function of the Cooper pair changes in response to the static Rydberg potential. This would require variational wave-function-based techniques, which is left for future research.

As seen in Figs. 2(b) and 2(c), intact trapping or breaking of a Cooper pair leads to distinct spectral profiles, either to a quasiparticle peak or to a power-law tail. The dimer state arises by breaking a Cooper pair, thus creating a Bogoliubov particle-hole excitation across the superconducting gap. Analogous to excitations in a semiconductor, the possible configurations of this particle-hole excitation in the dispersion lead to the characteristic tail seen in the dimer spectrum. In contrast, in the case of intact Cooper-pair trapping, additional particle-hole excitations are suppressed by the BCS gap, leading to the emergence of a quasiparticle peak.

Orthogonality catastrophe—We now show that Rydberg impurities in a BCS superfluid allow one to study the stabilization of quasiparticle behavior by emerging many-body energy gaps. In Fig. 2(d), we show the spectrum of the excited branch, where no bound state is occupied, for different gap strengths; we refer to this branch as the atomic Rydberg peak. At $\Delta = 0$, the characteristic power-law decay of an immobile impurity can be observed, which is not affected by the microscopic details of the scattering potential [24,25]. However, as the gap increases, the spectrum loses this attribute. Instead, the spectrum deforms from a power law into a broadened δ-like quasiparticle peak structure which we attribute to the gapped dispersion of the BCS bath suppressing low-energy particle-hole excitations. The gapped dispersion allows for a clear distinction of the physical mechanisms associated with the trimer and dimer peaks. When trapping an intact Cooper pair, low-energy excitations in the bath are suppressed by the energy gap, which results in the sharp trimer peak. On the other hand,

disrupting a Cooper pair leads to Bogoliubov excitations, which characterize the tail of the dimer peak. Indeed, the superfluid gap plays an analogous role to a mass gap generated by impurity recoil in the case of a mobile impurity in a Fermi sea [27]. In the Ramsey signal [inset in Fig. 2(d)], this is captured by the nondecaying signals for $\Delta > 0$.

As the gap increases, the appearance of a secondary branch becomes visible. This branch is the result of the excitation of a Bogoliubov mode from the lower branch of the Bogoliubov dispersion into the upper branch. The excitation must overcome the separation between the branches of the dispersion, reflected by the 2Δ shift. As the gap increases, the excitation becomes energetically less favorable, and the upper branch loses spectral weight, which is transferred to the lower quasiparticle branch.

The gap parameter dictates the timescale on which the Ramsey signal starts to deviate from the power-law decay, or OC regime, and transitions into a dynamical regime associated with quasiparticle formation. This is analyzed in Fig. 3, where dashed lines show the timescales given by $\sim 1/\Delta$. In order to quantitatively study the impact of the gapped dispersion in the suppression of the OC and quasiparticle formation, we fit the Ramsey signal to the asymptotic form (solid lines in Fig. 3):

$$S(t \gtrsim 1/\Delta) \approx Z_B e^{i\omega_B t} + Z_\gamma e^{i\omega_\gamma t}. \tag{8}$$

Here, Z_B and Z_γ represent the quasiparticle weights of the atomic and Bogoliubov excitation peaks, respectively, with $2\Delta \approx |\omega_B - \omega_\gamma|$. As can be seen from Fig. 3, this

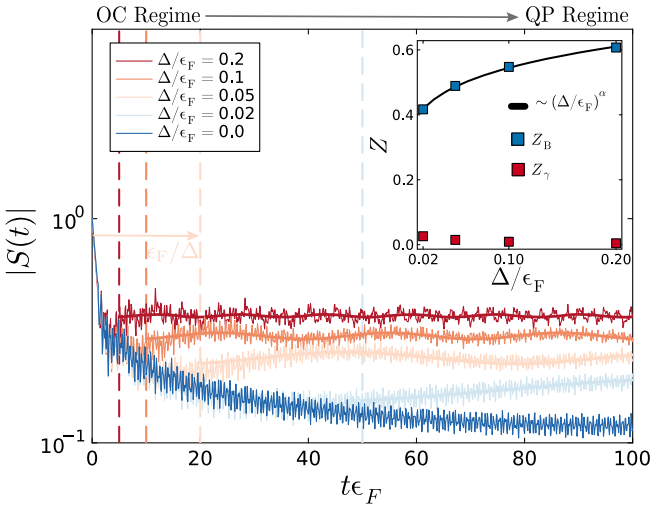


FIG. 3. Orthogonality catastrophe. Ramsey signal for different gap strengths showing the OC for $\Delta = 0$ and the emergence of a quasiparticle weight for $\Delta > 0$ where the signal is fitted (thick lines) to Eq. (8) at times $t \gtrsim 1/\Delta$ (dashed lines). Inset: quasiparticle weights of the bath and Bogoliubov excitation, where Z_B follows a power-law relation with scaling given by the scattering shift exponent [Eq. (9)].

fit describes the numerical data remarkably well. We find a power-law dependence of the quasiparticle weight of the bath with respect to the gap, leading to $Z_B^{(\Delta)} \sim (\Delta/\epsilon_F)^\alpha$ (see the inset in Fig. 3). This suppression of the orthogonality catastrophe has also been identified previously in a polaron-BCS system [28,29]. Here, we find that the scaling exponent is precisely given by

$$\alpha = \sum_\ell (2\ell + 1)\left[\frac{\delta_\ell(\epsilon_F)}{\pi}\right]^2, \tag{9}$$

where $\delta_\ell(\epsilon_F)$ is the scattering phase shift of the ℓ-scattering channel evaluated at the Fermi energy. Therefore, we recover the universal low-energy features of the OC [28,29] while simultaneously resolving the underlying dynamics of Cooper pairing at the microscopic level.

Conclusion—In this Letter, we demonstrated that Rydberg impurities can serve as a new comprehensive sensor to locally probe BCS superfluids. We have shown how the absorption spectrum provides critical insights into Cooper pairing, introducing an experimentally realizable tool to directly measure the gap parameter. Our real-time analysis further suggests that intact Cooper-pair trapping manifests as gap-independent spectral features with suppression of the orthogonality catastrophe and the emergence of a well-defined quasiparticle. The approach can be directly extended to study the dependence of the gap parameter on finite temperature and imbalanced mixtures. Future studies can extend this framework to explore the dynamics of a mobile impurity [27] and other strongly correlated systems. Moreover, to obtain more precise quantitative results in the strong-coupling regime, our mean-field BCS analysis may be extended by a self-consistent diagrammatic approach.

Acknowledgments—We thank Márton Kanász-Nagy for fruitful discussions. We acknowledge funding for E. R. R. and R. S. by the DFG (German Research Foundation)—Project No. 273811115—SFB 1225 ISOQUANT, the DFG Priority Programme of Giant Interactions in Rydberg Systems (GiRyd), and under Germany's Excellence Strategy No. EXC 2181/1-390900948 (the Heidelberg STRUCTURES Excellence Cluster). The authors acknowledge TU Wien Bibliothek for financial support through its Open Access Funding Programme.

Data availability—The data that support the findings of this article are not publicly available. The data are available from the authors upon reasonable request.

[1] I. Bloch, J. Dalibard, and W. Zwerger, Rev. Mod. Phys. **80**, 885 (2008).
[2] J. Bardeen, L. N. Cooper, and J. R. Schrieffer, Phys. Rev. **108**, 1175 (1957).

[3] A. Schirotzek, Y. I. Shin, C. H. Schunck, and W. Ketterle, Phys. Rev. Lett. **101**, 140403 (2008).
[4] S. Hoinka, P. Dyke, M. G. Lingham, J. J. Kinnunen, G. M. Bruun, and C. J. Vale, Nat. Phys. **13**, 943 (2017).
[5] H. Biss, L. Sobirey, N. Luick, M. Bohlen, J. J. Kinnunen, G. M. Bruun, T. Lompe, and H. Moritz, Phys. Rev. Lett. **128**, 100401 (2022).
[6] S. Kolkowitz, A. Safira, A. A. High, R. C. Devlin, S. Choi, Q. P. Unterreithmeier, D. Patterson, A. S. Zibrov, V. E. Manucharyan, H. Park, and M. D. Lukin, Science **347**, 1129 (2015).
[7] F. Casola, T. van der Sar, and A. Yacoby, Nat. Rev. Mater. **3**, 17088 (2018).
[8] W. Hofstetter, J. I. Cirac, P. Zoller, E. Demler, and M. D. Lukin, Phys. Rev. Lett. **89**, 220407 (2002).
[9] Q. Bouton, J. Nettersheim, D. Adam, F. Schmidt, D. Mayer, T. Lausch, E. Tiemann, and A. Widera, Phys. Rev. X **10**, 011018 (2020).
[10] N. Baldelli, B. Juliá-Díaz, U. Bhattacharya, M. Lewenstein, and T. Graß, Phys. Rev. B **104**, 035133 (2021).
[11] D. Adam, Q. Bouton, J. Nettersheim, S. Burgardt, and A. Widera, Phys. Rev. Lett. **129**, 120404 (2022).
[12] E. Urban, T. A. Johnson, T. Henage, L. Isenhower, D. D. Yavuz, T. G. Walker, and M. Saffman, Nat. Phys. **5**, 110 (2009).
[13] C. H. Greene, A. S. Dickinson, and H. R. Sadeghpour, Phys. Rev. Lett. **85**, 2458 (2000).
[14] B. J. DeSalvo, J. A. Aman, F. B. Dunning, T. C. Killian, H. R. Sadeghpour, S. Yoshida, and J. Burgdörfer, Phys. Rev. A **92**, 031403(R) (2015).
[15] M. T. Eiles, J. Phys. B **52**, 113001 (2019).
[16] C. Fey, F. Hummel, and P. Schmelcher, Mol. Phys. **118**, e1679401 (2020).
[17] M. Schlagmüller, T. C. Liebisch, H. Nguyen, G. Lochead, F. Engel, F. Böttcher, K. M. Westphal, K. S. Kleinbach, R. Löw, S. Hofferberth *et al.*, Phys. Rev. Lett. **116**, 053001 (2016).
[18] J. Sous, H. R. Sadeghpour, T. C. Killian, E. Demler, and R. Schmidt, Phys. Rev. Res. **2**, 023021 (2020).
[19] M. Gievers, M. Wagner, and R. Schmidt, Phys. Rev. Lett. **132**, 053401 (2024).
[20] C.-C. Chien, S. I. Mistakidis, and H. R. Sadeghpour, Phys. Rev. A **110**, L051303 (2024).
[21] C.-C. Chien, S. T. Rittenhouse, S. I. Mistakidis, and H. R. Sadeghpour, Phys. Rev. A **111**, 043316 (2025).
[22] R. Schmidt, M. Knap, D. A. Ivanov, J.-S. You, M. Cetina, and E. Demler, Rep. Prog. Phys. **81**, 024401 (2018).
[23] J. Wang, AAPPS Bull. **33**, 20 (2023).
[24] P. W. Anderson, Phys. Rev. Lett. **18**, 1049 (1967).
[25] P. Nozières and C. T. d. Dominicis, Phys. Rev. **178**, 1097 (1969).
[26] M. Gievers, R. Schmidt, J. von Delft, and F. B. Kugler, Phys. Rev. B **111**, 085151 (2025).
[27] X. Chen, E. Dizer, E. R. Rodríguez, and R. Schmidt, Phys. Rev. Lett. **135**, 193401 (2025).
[28] J. Wang, X.-J. Liu, and H. Hu, Phys. Rev. A **105**, 043320 (2022).
[29] J. Wang, X.-J. Liu, and H. Hu, Phys. Rev. Lett. **128**, 175301 (2022).
[30] See Supplemental Material at http://link.aps.org/supplemental/10.1103/3js1-2zc1 for additional details; Supplemental Material includes Refs. [13,19,24,27–29,31–34].
[31] I. Klich, An elementary derivation of Levitov's formula, in *Quantum Noise in Mesoscopic Physics*, edited by Y. V. Nazarov (Springer Netherlands, Dordrecht, 2003), pp. 397–402.
[32] D. Benjamin, I. Klich, and E. Demler, Phys. Rev. Lett. **112**, 247002 (2014).
[33] M. Combescot and P. Nozières, J. Phys. USSR **32**, 913 (1971).
[34] D. J. Griffiths and D. F. Schroeter, *Introduction to Quantum Mechanics*, 3rd ed. (Cambridge University Press, Cambridge, England, 2018).
[35] N. Y. Du and C. H. Greene, Phys. Rev. A **36**, 971 (1987).
[36] V. Bendkowsky, B. Butscher, J. Nipper, J. P. Shaffer, R. Löw, and T. Pfau, Nature (London) **458**, 1005 (2009).
[37] B. Butscher, J. Nipper, J. B. Balewski, L. Kukota, V. Bendkowsky, R. Löw, and T. Pfau, Nat. Phys. **6**, 970 (2010).
[38] M. Cetina, M. Jag, R. S. Lous, I. Fritsche, J. T. Walraven, R. Grimm, J. Levinsen, M. M. Parish, R. Schmidt, M. Knap *et al.*, Science **354**, 96 (2016).
[39] J. Zeiher, R. van Bijnen, P. Schauß, S. Hild, J.-y. Choi, T. Pohl, I. Bloch, and C. Gross, Nat. Phys. **12**, 1095 (2016).
[40] K. Schönhammer, Phys. Rev. B **75**, 205329 (2007).
[41] J. L. Bohn, Phys. Rev. A **61**, 053409 (2000).
[42] I. I. Ryabtsev, I. I. Beterov, D. B. Tretyakov, V. M. Entin, and E. A. Yakshina, Phys. Usp. **59**, 196 (2016).
[43] S. Liberman and J. Pinard, Phys. Rev. A **20**, 507 (1979).
[44] G. Ferrari, M. Inguscio, W. Jastrzebski, G. Modugno, G. Roati, and A. Simoni, Phys. Rev. Lett. **89**, 053202 (2002).
[45] C. Ospelkaus, S. Ospelkaus, K. Sengstock, and K. Bongs, Phys. Rev. Lett. **96**, 020401 (2006).
[46] C. Chin, R. Grimm, P. Julienne, and E. Tiesinga, Rev. Mod. Phys. **82**, 1225 (2010).
[47] M. T. Eiles, Phys. Rev. A **98**, 042706 (2018).